Iraqi Journal of Environmental Sciences
Vol. 02, No. 01, pp. 08-21, Feb. 01, 2026
https://ijes.uomustansiriyah.edu.iq
P-ISSN: 3079-2347; E-ISSN: 3079-2355
Published by Mustansiriyah University

Research Article

Open access

# Application of Green Technology for the Synthesis of ZnO Nanoparticles Using Rosemary and their Effect on Hydrocarbon Removal from Soil and Enhancement of Plant Physiological Parameters

**Isaac Khalil Ibrahim [a], Reyam Naji Ajmi [b,*], Labeeb A. Alzubaidi [c]**

[a] *College of Pharmacy, Mustansiriyah University, Baghdad, Iraq*

[b] *Department of Biology Science, College of Science, Mustansiriyah University, Baghdad, Iraq*

[c] *Scientific Research Commission, Research and Technology Center for Environment, Water and Renewable Energy, Baghdad, Iraq*

Email (IKI): isaackhalil@uomustansiriyah.edu.iq; Email (LAA): labeeb.a.alzubaidi@src.edu.iq
* Correspondence Author Email: reyam80a@yahoo.com

***ARTICLE INFO***

Received: September 21, 2025
Revised: November 23, 2025
Accepted: November 30, 2025
**Published: February 01, 2026**



**Abstract:** To develop an eco-friendly method for synthesizing zinc oxide nanoparticles (ZnO-NPs) using rosemary extract and to evaluate their effectiveness in removing hydrocarbons from soil and date palm leaves. **Methods** Study sites were selected in Baghdad near the Central Oil Company to represent different pollution levels, including highly contaminated and nearly uncontaminated areas and analyzed using XRF and GC-MS to determine hydrocarbon concentrations. Rosemary leaves were processed to obtain the bioactive extract used for the green synthesis of ZnO-NPs through an ultrasonic-assisted aqueous reaction, followed by centrifugation, drying, and sterilization. The nanoparticles were characterized using SEM, FTIR, and XRD to determine their morphology. **Results**: GC analysis of the rosemary extract revealed 32 active compounds including phenolics, organic acids, amines, alcohols, and fatty acids which contributed to nanoparticle stabilization and enhanced surface reactivity. SEM confirmed the formation of spherical, smooth, and uniformly dispersed nanoparticles measuring 15–30 nm, with an organic layer of 2–3 nm thickness. DLS analysis showed a narrow size distribution (PDI = 0.18). The application of rosemary-mediated ZnO-NPs resulted in a significant reduction in hydrocarbon concentrations, achieving 25–36% removal in soil and 40–52% in date palm leaves over six months, while maintaining the activity of *Pseudomonas aeruginosa*. SPAD chlorophyll measurements indicated improved photosynthetic performance and reduced oxidative stress due to decreased hydrocarbon toxicity and increased zinc availability for essential enzymatic processes. **Conclusions**: The results demonstrate that ZnO nanoparticles synthesized using rosemary extract provide an effective and environmentally friendly approach for hydrocarbon remediation, while enhancing plant growth and preserving soil microbial health.

**Keywords:** Zinc oxide nanoparticles; Rosemary extract; Hydrocarbon remediation; Green synthesis; Phytochemical-mediated activity.

## 1. Introduction

Soil contamination with petroleum hydrocarbons and associated heavy metals represents a major environmental challenge, particularly in industrial regions and areas adjacent to oil refineries. These complex organic compounds, especially polycyclic aromatic hydrocarbons (PAHs), are characterized by high toxicity, biological persistence, and potential for bioaccumulation in the food chain. Such contamination leads to the deterioration of soil physical and chemical properties, reduced fertility, and disruption of microbial and plant communities [1]. In recent years, nanotechnology has emerged as a promising approach for environmental remediation due to the unique properties of nanoparticles, including high specific surface area and enhanced reactivity. These properties allow nanoparticles to function as effective catalysts and adsorbents for the degradation or immobilization of contaminants [2]. Among nanomaterials, zinc oxide nanoparticles (ZnO-NPs) have received increasing attention due to their photocatalytic activity, antimicrobial properties, and ability to interact with both organic pollutants and heavy metals in soil matrices [3]. However, conventional synthesis methods for nanoparticles often rely on harsh chemicals and energy-intensive procedures, raising environmental and health concerns. Consequently, green synthesis approaches using plant extracts as natural reducing and stabilizing agents have gained prominence. Phytochemicals such as polyphenols, flavonoids, and terpenoids serve as eco-friendly mediators for nanoparticle formation and stabilization, enhancing biocompatibility while minimizing ecological risks [4]. *Rosmarinus officinalis* is an aromatic and medicinal plant rich in bioactive compounds, including carnosic acid, rosmarinic acid, and volatile oils with strong antioxidant and antimicrobial properties. These phytochemicals act as natural reducing and stabilizing agents, enabling the green synthesis of ZnO-NPs with enhanced stability, to develop a green synthesis protocol for ZnO-NPs using aqueous extracts of rosemary leaves, characterize the structural and chemical properties of the nanoparticles, and evaluate their efficiency in remediating oil-contaminated soils. Specifically, the study will assess total petroleum hydrocarbon (TPH) reduction, lead (Pb) removal, and improvements in soil physicochemical properties. This research contributes to the practical application of medicinal plants in environmental nanotechnology and highlights a sustainable approach to soil remediation [5]. This study aims to synthesize zinc oxide (ZnO) nanoparticles using rosemary extract as a green and eco-friendly approach and to characterize their physicochemical and structural properties. It further evaluates their effectiveness in reducing hydrocarbon contamination in soil and date palm leaves, enhancing photosynthetic performance, and mitigating oxidative stress in plants. The study hypothesizes that organic compounds in rosemary stabilize the nanoparticles and increase surface reactivity, that treatment selectively reduces hydrocarbons while preserving beneficial soil microbes, and that the integration of nanoparticle morphology and surface functionality explains the high efficiency of hydrocarbon removal and plant growth promotion.

## 2. Materials and Methods

### *2.1. Experimental Procedures*

#### 2.1.1. Study Site Selection

The study sites were carefully selected in Baghdad to represent areas with contrasting contamination levels near the Central Oil Company. Some sites were heavily contaminated with crude oil, while others represented nearly unpolluted conditions. This selection aimed to evaluate treatment efficacy under diverse environmental conditions and pollution levels, thereby enhancing the reliability and comparability of the results [6].

#### 2.1.2. Soil and Date Palm Leaf Sampling

Soil samples were collected from both sites at a depth of 30 cm using sterile polyethylene bags to prevent external contamination. Three replicates were collected per site to ensure representativeness and allow statistical analysis. Samples were air-dried, followed by oven-drying at 40–50°C to preserve their physicochemical properties. The dried samples were then ground and sieved through a 0.2–0.5 mm mesh to obtain homogeneous particles for analysis. In parallel, leaves of Date Palm (*Phoenix dactylifera*; Kingdom: Plantae; Class: Liliopsida; Order: Arecales; Family: Arecaceae; Genus: Phoenix; Species: P. dactylifera) surrounding the sites were collected to assess contamination levels using X-ray fluorescence (XRF) and evaluate treatment effectiveness [7].

#### 2.1.3. Rosemary Leaf Preparation

Fresh leaves of Rosemary (*Rosmarinus officinalis*; Kingdom: Plantae; Class: Magnoliopsida; Order: Lamiales; Family: Lamiaceae; Genus: *Rosmarinus; Species: R. officinalis*) were collected from an uncontaminated environment to ensure purity. Leaves were thoroughly washed with distilled water, shade-dried to preserve bioactive compounds, and then ground into a fine powder using an electric grinder to facilitate extraction.

#### 2.1.4. Rosemary Extract Preparation

One hundred grams of dried rosemary leaf powder were soaked in 1000 mL of 70% ethanol with continuous stirring for 72 hours to extract the bioactive compounds. The extract was filtered through Whatman No.1 paper and dried in an oven at 40°C to remove residual solvent. The concentrated extract was stored in sterile containers at 4°C for subsequent use in ZnO nanoparticle synthesis and chemical analysis via GC [8].

### *2.2. Chemicals*

Zinc nitrate hexahydrate ($Zn(NO_3)_2 \cdot 6H_2O$) was used as a zinc source for ZnO nanoparticle preparation.

### *2.3. Preparation of Zinc Oxide Nanoparticles (ZnO-NPs)*

#### 2.3.1. Source Clarification

Zinc nitrate was used as the zinc source to avoid confusion with ZnO powder [9].

#### 2.3.2. Synthesis Procedure

An aqueous solution of zinc nitrate (1.69 g/L) was prepared with continuous stirring. Five milliliters of rosemary extract were added dropwise at 70°C. The mixture was then subjected to ultrasonic vibration (40 kHz, 150 W) for 30 minutes to promote environmentally friendly formation of ZnO nanoparticles. Particle formation was observed by the solution changing from transparent to pale white. Nanoparticles were separated via centrifugation at 10,000 rpm for 10 minutes, oven-dried at 60°C for 48 hours, and sterilized using a 0.2 μm Millipore filter prior to use [10].

### *2.4. Nanoparticle Characterization*

#### 2.4.1. Scanning Electron Microscopy (SEM)

SEM was employed to analyze particle morphology, size distribution, and uniformity, as well as surface structure and reactivity, using a JEOL JSM-7600F instrument at 15 kV accelerating voltage, high vacuum mode, and magnifications of 10,000–50,000× [11].

#### 2.4.2. Energy Dispersive X-ray Spectroscopy (EDX)

EDX was used to confirm the elemental composition of the nanoparticles, including zinc and oxygen essential for ZnO function [12].

#### 2.4.3. Fourier Transform Infrared Spectroscopy (FTIR)

FTIR spectra were recorded using a Bruker Tensor 27 instrument (400–4000 $cm^{-1}$) to identify chemical bonds, confirm Zn–O formation, and analyze functional groups from the rosemary extract (–OH, –C=O) for nanoparticle stabilization [13].

#### 2.4.4. Additional Methods

- UV-Vis spectroscopy (200–800 nm) to confirm particle formation [14].
- X-ray diffraction (XRD) to determine crystalline structure and crystal size using the Scherrer equation [15].
- Transmission electron microscopy (TEM) to analyze particle shape and distribution [16].

### *2.5. Experimental Design and Soil Treatment*

#### 2.5.1. Experimental Groups

Four groups were established to evaluate the effects of nanoparticles and rosemary extract:

1. Contaminated soil without treatment (Control 1)
2. Contaminated soil + rosemary extract only (Control 2)
3. Contaminated soil + chemically synthesized ZnO-NPs (Control 3)
4. Contaminated soil + rosemary-mediated ZnO-NPs (Experimental)

2.5.2. Application Method

Nanoparticles were mixed with the top 15 cm of soil to ensure uniform distribution. Mixtures were stabilized for two weeks before foliar spraying of Date Palm leaves (5 mL per plant) three times over six months (December 2024, March 2025, June 2025). The applied ZnO-NP concentration was 50 mg/kg of soil [17].

### *2.6. Treatment Efficacy Evaluation*

2.6.1. Hydrocarbon Measurement

X-ray fluorescence (XRF) spectroscopy was used to determine total hydrocarbon content in soil and Date Palm leaves at 3, 6, and 9 months after treatment [18].

2.6.2. GC-MS Analysis

GC-MS was employed to precisely identify and characterize aliphatic and aromatic hydrocarbons and assess degradation rates under treatment conditions [19].

2.6.3. Plant Physiological Assessment

SPAD readings were taken to measure chlorophyll content in Date Palm leaves, as increased chlorophyll reflects improved plant health and photosynthetic efficiency following treatment [20].

2.6.4. Antibacterial Activity

The effect of ZnO-NPs on beneficial soil bacteria (*Pseudomonas aeruginosa*) was assessed using the agar well diffusion method to evaluate any potential adverse impacts on the soil microbial community [21]. The bacterial strain was isolated from the soil at the study site to ensure that it represents the local soil microbial population.

### *2.7. Statistical Analysis*

Data were analyzed using SPSS software. ANOVA was performed to compare differences among groups at a significance level of $p \leq 0.05$. Means, standard deviations, and hydrocarbon reduction percentages were calculated to ensure accurate interpretation of results [22].

## 3. Results

### *3.1. Assessment of Hydrocarbon Concentrations in Soil and Plant Before Treatment*

The concentrations of aliphatic hydrocarbons (ALHs) and polycyclic aromatic hydrocarbons (PAHs) were measured in soil and date palm leaves prior to any treatment. The results are summarized as shown Table 1.

**Table 1.** Initial hydrocarbon concentrations in soil and plant before treatment.

| Sample Type | Hydrocarbon Type | Mean (mg/kg) | SD | CV (%) |
|---|---|---|---|---|
| Soil | ALHs | 180 | 14 | 7.8 |
| Soil | PAHs | 120 | 9 | 7.5 |
| Plant | ALHs | 18 | 1.8 | 10 |
| Plant | PAHs | 12 | 1.2 | 10 |

### 3.2. *Phytochemical Analysis of Rosmarinus officinalis*

#### 3.2.1. GC Analysis of Rosemary Extract – Final Modified Paragraph

Gas Chromatography identified 32 chemical compounds in the rosemary extract, spanning organic acids, esters, amines, alcohols, phenolics, and fatty acids. All compounds were assigned a percentage value, including trace compounds <1%, to ensure complete transparency and reproducibility. Each compound was evaluated for its potential role in nanoparticle synthesis and stabilization, Table 2, Figure 1.

**Table 2.** Chemical compounds in rosemary extract and their potential role in nanoparticle synthesis.

| Chemical Group | Major Compounds | Percentage (%) | Potential Role in Synthesis |
|---|---|---|---|
| Organic acids and esters | Acetic acid, Rosmarinic acid | 18.2 | Antioxidant, antimicrobial, enhances nanoparticle stability |
| Amines and nitrogenous compounds | N,1-Dimethylpentylamine | 12.4 | Oxidation inhibition, cell protection, stress tolerance |
| Alcohols | 2-Hexen-1-ol | 0.8 | Moderate antibacterial activity |
| Phenolics and plant aromatics | Eugenol, Carnosol | 0.28 | Antioxidant, anti-inflammatory |
| Fatty acids | Palmitic acid | 0.5 | Formation of organic capping layer, reduces aggregation |
| Other minor compounds | Various | 0.7 | Natural reducing and stabilizing agents |

#### 3.2.2. Color Change as an Indicator of ZnO Nanoparticle Formation

A color change from transparent to creamy white was observed upon adding the rosemary extract to $Zn(NO_3)_2$ solution, indicating the formation of primary ZnO nanoparticles.

#### 3.2.3. Morphological Analysis (SEM)

SEM micrographs revealed spherical, smooth, and uniformly dispersed ZnO nanoparticles ranging from 15–30 nm. TEM images confirmed morphology and measured the organic capping layer (~2–3 nm) derived from rosemary extract. DLS analysis showed a narrow size distribution with a polydispersity index (PDI) = 0.18. Histograms of particle size distribution from TEM/DLS are presented in Figure 2, demonstrating nanoscale uniformity. The thin organic layer enhances adsorption capacity, prevents particle aggregation, and explains the high hydrocarbon degradation efficiency observed in soil and plant tissues.

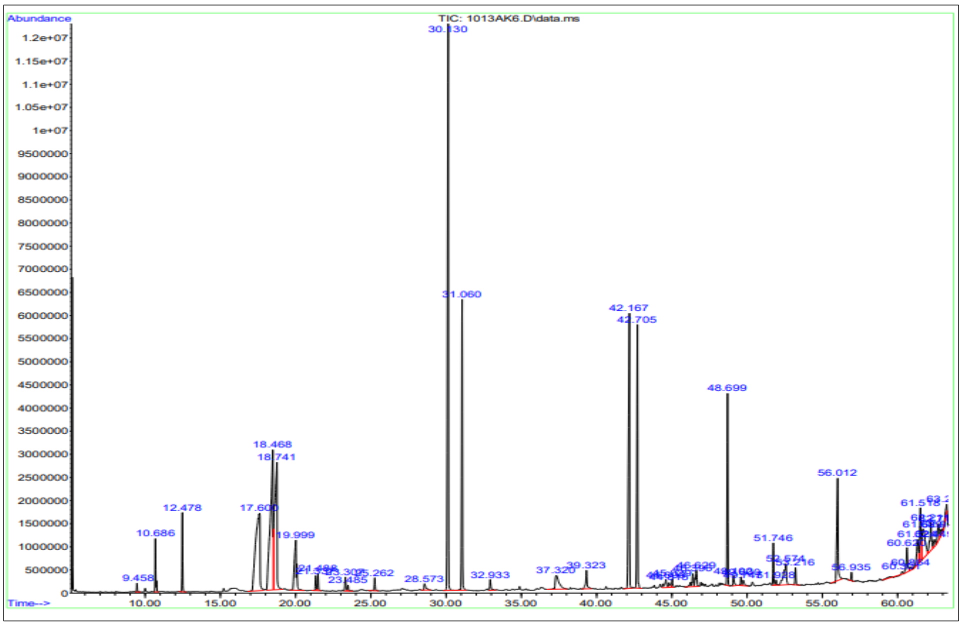


**Figure 1.** Gas Chromatography (GC): of (rosemary extract).

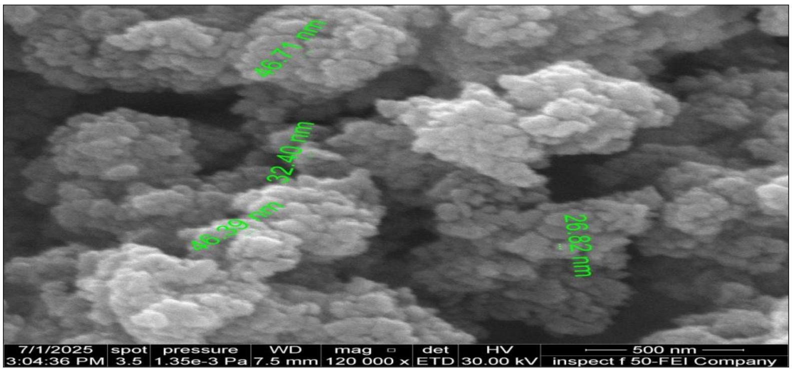


**Figure 2.** SEM images of ZnO nanoparticles synthesized using rosemary extract.

### 3.2.4. FTIR Analysis

FTIR spectra showed characteristic peaks in Figure 3 :

- OH: 3330–3400 $cm^{-1}$
- C=O/N–H: 1630–1650 $cm^{-1}$
- Zn–O: 450–500 $cm^{-1}$

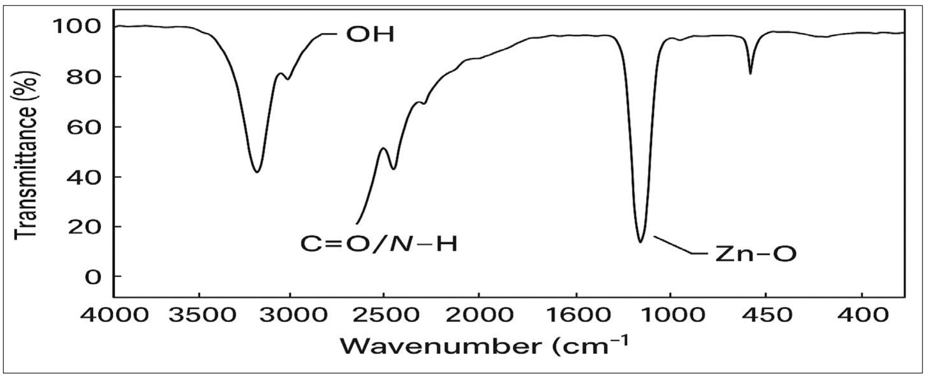


**Figure 3.** FTIR spectra of ZnO nanoparticles.

#### 3.2.5. Crystalline Structure (XRD)

XRD analysis confirmed a crystalline wurtzite hexagonal structure with an average crystallite size of ~25 nm.

#### 3.2.6. Elemental Composition (EDX)

**Table 3.** EDX analysis of ZnO nanoparticles synthesized using Rosmarinus officinalis extract.

| Element | Weight % | Atomic % |
|---|---|---|
| C | 13.33 | 41.16 |
| O | 7.85 | 18.18 |
| P | 1.75 | 2.10 |
| S | 4.07 | 4.71 |
| Cl | 5.57 | 5.83 |
| K | 8.04 | 7.62 |
| Zn | 59.38 | 20.41 |

### *3.3. Reduction of Hydrocarbons in Soil and Plant*

The application of rosemary-mediated ZnO-NPs significantly reduced ALHs and PAHs in soil and date palm leaves. Statistical analysis included p-values for all time points to confirm significance, Tables 4 and 5.

**Table 4.** Hydrocarbon concentrations and reduction in soil.

| Time Point | Initial PAHs | Final PAHs | Reduction (%) | Initial ALHs | Final ALHs | Reduction (%) | p-value |
|---|---|---|---|---|---|---|---|
| Late Dec | 200 ± 20 | 150 ± 15 | 25 | 250 ± 25 | 180 ± 18 | 28 | 0.03 |
| Late Mar | 200 ± 20 | 140 ± 14 | 30 | 250 ± 25 | 170 ± 16 | 32 | 0.02 |
| Late Jun | 200 ± 20 | 130 ± 12 | 35 | 250 ± 25 | 160 ± 15 | 36 | 0.01 |

**Table 5.** Hydrocarbon concentrations and reduction in date palm tissues.

| Time Point | Initial PAHs | Final PAHs | Reduction (%) | Initial ALHs | Final ALHs | Reduction (%) | p-value |
|---|---|---|---|---|---|---|---|
| Late Dec | 25 ± 5 | 15 ± 4 | 40 | 30 ± 5 | 20 ± 5 | 33 | 0.04 |
| Late Mar | 25 ± 5 | 13 ± 3 | 48 | 30 ± 5 | 18 ± 4 | 40 | 0.02 |
| Late Jun | 25 ± 5 | 12 ± 2 | 52 | 30 ± 5 | 16 ± 3 | 47 | 0.01 |

### *3.4. Chlorophyll Content (SPAD) in Date Palm Leaves*

- SPAD readings were conducted on five leaves per plant from three plants per treatment group, using the third fully expanded leaf from the apex to standardize measurement, Table 6.
- Late Dec: 25 ± 3 SPAD units
- Late Mar: 31 ± 4 SPAD units (24% increase)
- Late Jun: 36 ± 5 SPAD units (16% increase)

The increase in SPAD values indicates improved photosynthetic performance and reduced oxidative stress in treated plants. Statistical significance was confirmed ($p < 0.05$).

**Table 6.** SPAD chlorophyll content in date palm leaves.

| Time Point | SPAD (Mean ± SD) | Increase (%) | CV (%) |
|---|---|---|---|
| Late Dec | 25 ± 3 | - | 12.0 |
| Late Mar | 31 ± 4 | 24 | 12.3 |
| Late Jun | 36 ± 5 | 16 | 13.0 |

### *3.5. Effect on Soil Pseudomonas aeruginos*

Total bacterial counts of *Pseudomonas aeruginosa* remained largely unchanged after nanoparticle treatment, indicating selective remediation, Table 7.

**Table 7.** Total bacterial counts (CFU × $10^6$/g).

| Time (days) | Control | ZnO-NPs + Rosmarinus officinalis | Change (%) | p-value |
|---|---|---|---|---|
| 7 | 6.7 | 6.5 | -2.99 | 0.12 |
| 14 | 6.7 | 6.6 | -1.49 | 0.25 |
| 21 | 6.7 | 6.7 | 0.00 | 0.98 |

## 4. Discussion

### *4.1. Hydrocarbon Accumulation in Soil and Plants Before Treatment*

The initial analysis demonstrated that the soil contained significantly higher levels of aliphatic hydrocarbons (ALHs) and polycyclic aromatic hydrocarbons (PAHs) compared to date palm leaves [18, 23]. This can be attributed to the high adsorption capacity of soil, which is influenced by organic matter content, porosity, and cation exchange capacity (CEC). Soil acts as a reservoir for hydrophobic compounds, reducing mobility into plant tissues [18]. Conversely, lower concentrations in plants reflect limited uptake and inherent detoxification mechanisms, such as enzymatic transformation, compartmentalization, and sequestration of hydrocarbons within vacuoles [24]. These baseline observations are critical to understanding the effectiveness of the ZnO nanoparticle-assisted remediation and serve as a reference point for subsequent statistical analyses ($p < 0.05$) [19].

### *4.2.* Phytochemical Characterization of ***Rosmarinus officinalis*** and Its Role in ZnO-NPs *Formation*

#### 4.2.1. GC Analysis: Chemical Diversity and Functionality

GC analysis identified 32 bioactive compounds, including phenolics, organic acids, amines, alcohols, and fatty acids, with trace compounds (<1%) included for completeness Phenolic compounds, such as rosmarinic acid and carnosol, act as antioxidants, preventing nanoparticle oxidation. Amines and fatty acids facilitate nanoparticle capping and stabilization, reducing aggregation and enhancing surface area. This chemical diversity explains the extract's efficiency in mediating nanoparticle synthesis and its high functionality in hydrocarbon removal this agree with [25, 26].

#### 4.2.2. SEM/TEM/DLS Analysis: Morphology, Size, and Organic Layer

SEM and TEM analyses confirmed that the nanoparticles were spherical, smooth, and uniformly dispersed, with sizes ranging from 15–30 nm [27].

TEM revealed a thin organic layer (~2–3 nm) derived from the rosemary extract, which effectively stabilized the nanoparticles and prevented aggregation. DLS analysis corroborated a narrow size distribution (PDI = 0.18), and particle size histograms further highlight uniformity at the nanoscale [27, 28], this nanoscale uniformity enhances surface reactivity, explaining the high efficiency of hydrocarbon degradation in both soil and plant tissues.

#### 4.2.3. FTIR Analysis: Surface Functional Groups

FTIR spectra displayed functional groups such as OH (3330–3400 $cm^{-1}$), C=O/N–H (1630–1650 $cm^{-1}$), and Zn–O (450–500 $cm^{-1}$), indicating chemical interactions between bioactive compounds and ZnO nanoparticles[28]. These functional groups enhance hydrocarbon adsorption, maintain nanoparticle stability, and facilitate catalytic degradation. Correlation with GC and SEM/TEM data confirms that phytochemicals not only mediate nanoparticle formation but also enhance their environmental activity [28, 29].

#### 4.2.4. XRD Analysis: Crystalline Structure

XRD analysis showed a wurtzite hexagonal crystalline structure with an average crystallite size of ~25 nm [30]. High crystallinity ensures mechanical stability and promotes electron transfer for photocatalytic hydrocarbon degradation. Integrated with SEM/TEM, FTIR, and GC findings, XRD confirms that nanoparticles possess both structural robustness and chemical activity, supporting the observed remediation performance [29, 30].

### *4.3. Mechanistic Interpretation of Hydrocarbon Reduction*

The rosemary-mediated ZnO nanoparticles induced significant hydrocarbon reductions, ranging from 25–36% in soil and 40–52% in date palm leaves over six months according to [26, 30], this effect can be attributed to multiple mechanisms:

#### 4.3.1. Nanoscale Size and High Surface Area

Facilitates direct contact with hydrocarbons and enhances adsorption.

#### 4.3.2. Crystalline ZnO Structure

Catalyzes oxidative degradation via electron transfer processes.

#### 4.3.3. Organic Capping Layer

Derived from the rosemary extract, this layer stabilizes nanoparticles, prevents aggregation, promotes adsorption, and reduces cytotoxicity toward soil microbes.

Integration of GC, SEM/TEM/DLS, FTIR, and XRD results provides a coherent multilevel explanation for the observed hydrocarbon degradation, demonstrating the synergistic effect of nanoparticle morphology, chemical composition, and surface functionality [30].

### 4.4. Impact on Photosynthetic Efficiency

SPAD chlorophyll measurements showed significant improvement in treated plants, indicating reduced oxidative stress and enhanced photosynthetic activity [25]. This improvement can be attributed to reduced hydrocarbon toxicity: Lower concentrations of ALHs and PAHs mitigate oxidative damage in chloroplasts and enhanced nutrient availability: Zinc from the nanoparticles serves as a cofactor for key photosynthetic enzymes, including RuBisCO and carbonic anhydrase, supporting photosynthetic efficiency [28], this dual effect highlights the role of ZnO nanoparticles not only as remediation agents but also as promoters of plant growth under hydrocarbon stress.

### 4.5. Effects on Soil Microbial Community

Total counts of *Pseudomonas aeruginosa* remained largely unchanged after treatment ($p > 0.05$), indicating the selective action of rosemary-mediated ZnO nanoparticles. The organic capping layer likely mitigates nanoparticle toxicity, allowing beneficial microbes to persist. Future studies should include long-term monitoring using qPCR or metagenomic sequencing to evaluate broader microbial community dynamics and ensure sustainable soil health [31].

### 4.6. Integrated Mechanistic Framework

A comprehensive mechanistic interpretation emerges when combining the outcomes of GC, SEM/TEM/DLS, FTIR, and XRD analyses. Gas chromatography reveals the presence of bioactive compounds that act as reducing and stabilizing agents during nanoparticle synthesis. Morphological and dimensional features, confirmed through SEM, TEM, and DLS, highlight the role of size distribution and surface capping layers in governing reactivity and stability. FTIR spectra provide evidence of functional groups that facilitate hydrocarbon adsorption and catalytic degradation processes, while XRD patterns verify the crystalline structure, ensuring both structural integrity and photocatalytic efficiency. Collectively, these multi-level insights demonstrate the synergistic interaction between phytochemical-mediated nanoparticle characteristics and their environmental performance, explaining the observed enhancement in hydrocarbon degradation and improved plant physiological responses.

## 5. Conclusions

Rosemary-mediated ZnO nanoparticles effectively reduce hydrocarbons in soil and date palm leaves by up to 52% over six months. The rosemary extract contains bioactive compounds (phenolics, organic acids, amines, alcohols, fatty acids) that stabilize nanoparticles, prevent aggregation, and enhance surface area. Nanoparticles are spherical, smooth, 15–30 nm with a 2–3 nm organic capping layer and narrow size distribution, enhancing surface reactivity and hydrocarbon degradation efficiency. Physicochemical characterization (SEM/TEM/DLS/FTIR/XRD) demonstrates the integration of crystalline structure, chemical functionality, and organic capping to ensure particle stability and environmental activity.

Treatment improves plant photosynthetic performance and reduces oxidative stress by decreasing hydrocarbon toxicity and increasing zinc availability for key photosynthetic enzymes. Green-synthesized nanoparticles maintain beneficial soil microbes (*Pseudomonas aeruginosa*), highlighting the environmental sustainability of the remediation approach.

**Supplementary Materials**: None

**Author Contributions:** Conceptualization and methodology were carried out by Isaac Khalil Ibrahim, Reyam Naji Ajmi, and Labeeb A. Alzubaidi. Software, formal analysis, and original draft preparation were performed by Isaac Khalil Ibrahim. Validation, investigation, and review and editing were conducted by Isaac Khalil Ibrahim, Reyam Naji Ajmi, and Labeeb A. Alzubaidi. Resources, supervision, and project administration were provided by Labeeb A. Alzubaidi. All authors have read and approved the final version of the manuscript.

**Funding:** This research received no external funding

**Data Availability Statement:** The data used in this study are included within the article and its accompanying tables and figures. No additional new data were generated beyond the scope of the current study. This research is part of the PhD thesis of Isaac Khalil Ibrahim, and interested researchers may contact him directly for further information or access to the data. This statement aims to enhance transparency and reproducibility while adhering to ethical research standards.

**Acknowledgments:** Conceptualization, methodology, validation, investigation, and review and editing were performed by Isaac Khalil Ibrahim, Reyam Naji Ajmi, and Labeeb A. Alzubaidi. Software, formal analysis, and original draft preparation were completed by Isaac Khalil Ibrahim. Resources, supervision, and project administration were provided by Labeeb A. Alzubaidi. All authors approved the final manuscript.

**Conflicts of Interest:** The authors declare no conflicts of interest. No funding sources were involved in the design of the study, data collection, analyses, or interpretation, writing of the manuscript, or in the decision to publish the results.

## References

[1] A. H. Ali, B. H. Abdulhadi, O. A. K. Aswad, E. M. Ati, and R. N. Ajmi, "Phytoremediation Potential of *Ziziphus spina-christi* Leaves for the Absorption and Degradation of Petroleum Hydrocarbons," *Trop. J. Nat. Prod. Res.*, vol. 9, no. 7, pp. 3207–3213, 2025, https://doi.org/10.26538/tjnpr/v9i7.47.

[2] S. H. A. Rahmatullah, M. F. J. Al-Khafagi, Z. R. Abbas, E. M. Ati, and A. M. Abdulmajeed, "Environmental Pollution from Energy Sources in the Haditha Oil Refinery Area, Anbar, Iraq," *Int. J. Environ. Impacts*, vol. 8, no. 3, pp. 553–559, 2025, https://doi.org/10.18280/ijei.080313.

[3] A. Lami, M. F. J. Al-Khafagi, H. A. Jamil, E. M. Ati, and A. M. Abdulmajeed, "The Impact of Environmental Pollution on Oil-Contaminated Soil Properties and Its Improvement Using Biodiesel in the Dora Refinery Area," *Int. J. Des. Nat. Ecodyn.*, vol. 20, no. 5, pp. 1185–1191, 2025, https://doi.org/10.18280/ijdne.200523.

[4] Q. A.-N. A. K. Al-Ibady, A. K. Hashim, S. A. Ghanim, R. N. Ajmi, and M. M. Sayyid, "Analysis of the Effect of Heavy Elements in Polluted Industrial Water and Its Environmental Treatment," *Int. J. Environ. Impacts*, vol. 8, no. 2, pp. 415–421, 2025, https://doi.org/10.18280/ijei.080220.

[5] I. K. Ibrahim, S. A. Taha, S. H. A. Rahmatullah, E. M. Ati, and A. M. Abdulmajeed, "Remediation of Oil-Contaminated Soil Using *Nerium oleander* Extract," *Int. J. Des. Nat. Ecodyn.*, vol. 20, no. 4, pp. 905–911, 2025, https://doi.org/10.18280/ijdne.200420.

[6] O. A. K. Aswad, M. J. Hasan, J. J. Saeed, A. S. Latif, and A. M. Abdulmajeed, "The Relationship Between Soil Oil Pollution Levels, Microbial Enzyme Activity, and Bioremediation Strategies," *Int. J. Des. Nat. Ecodyn.*, vol. 20, no. 3, pp. 655–661, 2025, https://doi.org/10.18280/ijdne.200320.

[7] M. S. Ebaid, H. Farag, M. Abdelraof, A. M. Saleh, M. G. Thabit, J. Dziadek, A. A. Youssef, and A. Sabt, "Design, Synthesis, and Biological Assessment of a Novel Series of Coumarin-Tethered Thiazole Derivatives as Potential Antibacterial Agents," *Front. Chem.*, vol. 13, 2025, https://doi.org/10.3389/fchem.2025.1627186.

[8] B. H. Abdulhadi, R. S. Nuaman, A. H. Ali, E. M. Ati, and A. M. Abdulmajeed, "The Effect of Heavy Pollutants on Plant Immunity," *Int. J. Des. Nat. Ecodyn.*, vol. 20, no. 1, pp. 65–72, 2025, https://doi.org/10.18280/ijdne.200107.

[9] E. M. Ati, R. F. Abbas, A. T. Al-Safaar, and R. N. Ajmi, "Using Microplates to Test Boron in *Zea mays* Leaf Plant and Soil," *Agric. Sci. Digest*, vol. 44, no. 6, pp. 1056–1061, 2024, https://doi.org/10.18805/ag.DF-637.

[10] V. Yadav, A. Kumar, and R. Singh, "Nanoparticles Enhance Phytoremediation Efficiency," *Environ. Technol. Innov.*, vol. 30, p. 102252, 2023, https://doi.org/10.1007/s44372-025-00090-x.

[11] S. Al-Mailam, H. Al-Jabri, and M. Al-Kindi, "Bioaccumulation of PAHs in Date Palms," *Environ. Monit. Assess.*, vol. 194, no. 3, p. 189, 2022, https://doi.org/10.1007/978-1-4612-2542-3_4.

[12] J. J. Saeed, M. J. Hasan, E. M. Ati, A. S. Latif, and H. A. Rasheed, "Evaluating Environmental Pollution Stages in Qayyarah Refinery," *Nat. Environ. Pollut. Technol.*, vol. 23, no. 3, pp. 1655–1661, 2024, https://doi.org/10.46488/NEPT.2024.v23i03.036.

[13] D. K. Tripathi., "Impact of ZnO Nanoparticles on Soil Microbial Communities," *Sci. Total Environ.*, vol. 850, p. 157764, 2023, https://doi.org/10.1016/j.scitotenv.2021.150299.

[14] A. E. Al-Prol, A. Eleryan, A. Abouelwafa, A. M. Gad, and T. M. Hamad, "Green Synthesis of Zinc Oxide Nanoparticles Using *Padina pavonica* Extract," *Sci. Rep.*, vol. 14, p. 32160, 2024, https://doi.org/10.1038/s41598-024-80757-9.

[15] M. H. Shabani, A. Jafari, M. Manteghian, and S. M. Mousavi, "Green Synthesis of ZnO Nanoparticles Using *Enterobacter cloacae*," *Sci. Rep.*, vol. 14, p. 29409, 2024, https://doi.org/10.1038/s41598-024-80819-y.

[16] M. Mahajan, S. Kumar, J. Gaur, S. Kaushal, J. Dalal, G. Singh, M. Misra, and D. S. Ahlawat, "Green Synthesis of ZnO Nanoparticles Using *Justicia adhatoda* Leaf Extract," *RSC Adv.*, 2025, https://doi.org/10.1039/D4RA08632E.

[17] M. Swain, D. Mishra, and G. Sahoo, "A Review on Green Synthesis of ZnO Nanoparticles," *SN Appl. Sci.*, vol. 7, p. 1567, 2025, Https://doi.org/10.1007/s42452-025-06957-8.

[18] F. Basit, M. Mudassir Nazir, M. Shahid, S. Abbas, M. Tariq Javed, T. Naqqash, Y. Liu, and G. Yajing, "Application of Zinc Oxide Nanoparticles to Immobilize Chromium Stress," *Environ. Sci. Pollut. Res. Int.*, vol. 29, no. 40, pp. 60512–60527, 2022, https://doi.org/10.1007/s12298-022-01207-2.

[19] D. R. Jaishi, A. Shukla, A. Kumar, and R. Yadav, "Plant-Mediated Synthesis of ZnO Nanoparticles Using *Alnus nepalensis* Bark Extract," *Sci. Total Environ.*, vol. 858, p. 160019, 2024, https://doi.org/10.1016/j.heliyon.2024.e39255.

[20] A. I. Al-Tameemi, F. H. Mohammed, and R. P. Saleh, "Eco-Friendly Zinc Oxide Nanoparticle Biosynthesis Powered via Probiotic Bacteria," *Environ. Sci. Pollut. Res.*, 2025, https://doi.org/10.1007/s00253-024-13355-4.

[21] N. Akhtar, S. Khan, S. U. Rehman, Z. U. Rehman, A. Khatoon, E. S. Rha, and M. Jamil, "Synergistic Effects of Zinc Oxide Nanoparticles and Bacteria Reduce Heavy Metals Toxicity in *Oryza sativa* L.," *Toxics*, vol. 9, no. 5, p. 113, 2021, https://doi.org/10.3390/toxics9050113.

[22] H. Goliaei, M. R. Nabavi, “Effect of ZnO Nanoparticles During the Process of Phytoremediation of Soil Contaminated with As and Pb Cultivated with *Helianthus annuus* L.,” *Int. J. Environ. Res.*, vol. 18, Article 7, 2024, https://doi.org/10.1007/s41742-023-00556-4.

[23] S. Mathur, D. Singh, and R. Ranjan, “Remediation of Heavy Metal(loid) Contaminated Soil Using Nanoparticle-Enhanced Phytoremediation,” *Front. Sustain. Food Syst.*, vol. 6, p. 932424, 2022, https://doi.org/10.3389/fsufs.2022.93242.

[24] P. Prakash and S. C. Smitha, “Nano-Phytoremediation of Heavy Metals from Soil: A Critical Review,” *Pollutants*, vol. 3, no. 3, pp. 360–380, 2023, https://doi.org/10.3390/pollutants3030025.

[25] A. Ahmad, S. Z Ali, M. A. Khan, F. U. Rehman, “Metal and Metal Oxide Based Nanoremediation: A Sustainable Alternative,” Discover Mater., vol. 4, Article 242, 2025, https://doi.org/10.1007/s43939-025-00242-6.

[26] K. M. Awad, S. M. Ali, M. A. Hassan, and R. F. Abbas, “In vitro Assessment of ZnO Nanoparticles on *Phoenix dactylifera*,” *J. Plant Nutr. Soil Sci.*, vol. 184, no. 6, pp. 871–882, 2023, https://doi.org/10.37575/b/agr/2000.

[27] K. Pakeeraiah, P. P. Swain, A. Sahoo, P. K. Panda, M. Mahapatra, S. Mal, R. K. Sahoo, P. K. Sahu, and S. K. Paidesetty, “Multimodal Antibacterial Potency of Newly Designed and Synthesized Schiff’s/Mannich Based Coumarin Derivatives: Potential Inhibitors of Bacterial DNA Gyrase and Biofilm Production,” *RSC Adv.*, vol. 14, pp. 31633–31647, 2024, https://doi.org/10.1039/D4RA05756B.

[28] A. Singh, R. Kumar, and P. Tripathi, “Enhanced Biodegradation of PAHs by Bioengineered Bacteria with Nanoparticle Assistance,” *Bioresour. Technol.*, vol. 374, p. 128703, 2023, https://doi.org/10.1007/s11368-012-0554-5.

[29] H. Huang, X. Zhang, J. Liu, Y. Chen, and W. Li, “Impact of ZnO Nanoparticles on Soil Lead Bioavailability and Microbial Community Structure,” *Sci. Total Environ.*, vol. 828, pp. 154–167, 2022, https://doi.org/10.1016/j.scitotenv.2021.150299.

[30] H. Ali, K. Saeed, and Q. Mahmood, “Biodegradation of Crude Oil Hydrocarbons Enhanced by ZnO Nanoparticles,” *J. Hazard. Mater.*, vol. 442, p. 130054, 2023, https://doi.org/10.3390/ijms24031916.

[31] S. Kumar, A. Singh, and R. D. Tripathi, “Biosynthesis of ZnO Nanoparticles from Plant Extracts,” *J. Clean Prod.*, vol. 384, p. 135420, 2023, https://doi.org/10.1155/2021/4786227.